Research Paper
Computational Methods for Differential Equations
http://cmde.tabrizu.ac.ir
Vol. 14, No. 1, 2026, pp. 305-315
DOI:10.22034/cmde.2025.63589.2838

An efficient numerical solution of the optimal control mathematical models for pollutant spread through forest resources based on shifted Bernoulli polynomials

Asiyeh Ebrahimzadeh and Elham Keshavarz Hedayati*
Department of Mathematics Education, Farhangian University, P.O. Box 14665-889, Tehran, Iran.

Abstract

This study presents a computational method for solving a mathematical model of optimal control for pollutant spread through forest resources using shifted Bernoulli polynomials (SBPs). The model is formulated as an optimal control problem governed by a system of ordinary differential equations, which is then transformed into a nonlinear programming problem (NLP) using the collocation approach and operational matrix of derivatives based on SBPs. The NLP is employed to obtain numerical solutions, and the results demonstrate the proposed method's acceptability for modeling pollutant spread through forest resources. The study advises three controls on both types of industries (wood-based and non-wood-based) and forest resources to reduce pollution.

Keywords. Pollutants, Optimal control, Forest resources, Shifted Bernoulli polynomials, Collocation method.
2010 Mathematics Subject Classification. 49M25, 65L60, 93C15, 90C30, 92D40.

1. Introduction

The management and control of environmental pollution is a critical issue that has gained significant attention in recent years, particularly in the context of forest resources. Forests are essential for maintaining ecological balance and offering crucial ecosystem services, such as carbon sequestration, air purification, and habitat preservation [17]. However, the introduction of pollutants into forest ecosystems can disrupt these delicate systems, leading to the degradation of forest resources and the loss of biodiversity. The spread of pollutants through forest resources can occur through various pathways, including atmospheric deposition, surface water runoff, and groundwater contamination. Understanding and mitigating the dynamics of pollutant spread in forest environments is, therefore, a pressing challenge for environmental researchers and policymakers.

Developing efficient numerical solutions for the optimal control of pollutant spread is essential for effective environmental management and the preservation of forest resources [17]. The importance of this research topic is underscored by the significant environmental and economic impacts of pollutant spread in forest ecosystems. Pollutants can adversely affect the growth and health of forest vegetation, leading to the loss of valuable timber resources and the disruption of ecosystem services. Furthermore, the contamination of forest soils and water bodies can have far-reaching consequences, impacting the health and well-being of wildlife and human populations that depend on these resources [17]. The economic costs associated with the remediation and restoration of degraded forest environments can be substantial, highlighting the need for proactive and efficient strategies for the management of pollutant spread.

One prominent approach in the literature has been the use of systems of nonlinear ordinary differential equations to capture the relationships between key variables such as forest resource density, wood-based industries, non-wood-based industries, and associated pollutants [1, 17]. For example, the paper [17] formulated a model with five discrete compartments and derived the basic reproduction number R_0 using the next generation matrix method. Sensitivity analysis has also been a valuable tool in these modeling studies, allowing researchers to determine the impact of various model parameters on the spread of pollutants [2, 17]. Other works have explored the effects of toxicants,

Received: 18 September 2024; Accepted: 27 Febbruary 2025.
∗ Corresponding author. Email: e.keshavarz@cfu.ac.ir.

intermediate products, and the interactions between industrialization, population, and pollution on renewable resources [5, 12, 15, 16]. While these mathematical models have provided important insights, the numerical solution of the associated optimal control problems remains a challenge. Conventional numerical methods can be computationally intensive, especially for high-dimensional systems. To address this, some researchers have explored the use of advanced numerical techniques, such as those based on orthogonal polynomials. The use of Bernoulli polynomials for the numerical solution of optimal control problems has gained attention in recent years [6, 7].

In this context, the use of Bernoulli polynomials has emerged as a promising approach for modeling and solving optimal control problems related to pollutant spread. The main advantages of using Bernoulli polynomials to approximate solutions of complex systems are Computational simplicity, efficiency, and acceptable accuracy. Bernoulli polynomials have a simple, linear structure that makes the computations easy and efficient, which is particularly useful for complex systems with many variables. By selecting an appropriate degree for the Bernoulli polynomial, one can achieve a reasonably accurate approximation of the actual solution. In many cases, a low degree is sufficient [6, 8]. The efficient numerical solution of optimal control problems based on Bernoulli polynomials can provide environmental managers and decision-makers with a valuable tool for designing and implementing effective strategies for the mitigation and control of pollutant spread in forest resources. The proposed research aims to develop an efficient numerical solution for the optimal control of pollutant spread through forest resources based on Bernoulli polynomials and their operational matrix [14]. By using these polynomials and the collocation method, the optimal control problem of the forest resource was turned into a NLP. There are different optimization methods to solve this optimization problem [13]. The successful completion of this research will contribute to the existing body of knowledge in the field of optimal control and environmental management, providing a novel and efficient approach for addressing the critical issue of pollutant spread in forest resources.

The structure of this paper is as follows: Section 2 covers the introduction of mathematical models for pollutant spread through forest resources. Some basic definitions of shifted Bernoulli polynomials and their operational matrix of derivative are presented in section 3. Section 4 is devoted to the numerical approach for solving the mathematical modeling for pollutant spread through forest resources. Convergence analysis is given in section 6. In section 7, a numerical simulation is presented to demonstrate the practicality and precision of our method. Lastly, concluding remarks are proved.

2. Mathematical model

Mathematical modeling is a crucial process in science and engineering that helps us describe and predict real-world phenomena using mathematical tools. Mathematical modeling has wide applications in various scientific and engineering fields, including mechanics, electronics, economics, medicine, and more. This process helps us simplify and understand complex phenomena and make more accurate predictions. The mathematical models for pollutant spread through forest resources investigate and predict the way pollutants spread in forest environments. These models help researchers better understand the behavior of pollution in forests and develop methods to control and reduce pollution. This type of model is mentioned in [17], which we have included in the following problem:

Problem $\mathcal{A}$: Find the state-control function pair, $t \longrightarrow (x(t), u(t)) \in \mathbb{R}^5 \times \mathbb{R}^3$, for minimizing the cost function

$$\mathcal{J} = \int_0^L \left(A_1\mathcal{F}^2(t) + A_2\mathcal{W}^2(t) + A_3\mathcal{I}^2(t) + A_4\mathcal{P}_w^2(t) + A_5\mathcal{P}_I^2(t) + \omega_1\mathcal{U}_1^2(t) + \omega_2\mathcal{U}_2^2(t) + \omega_3\mathcal{U}_3^2(t)\right) dt, \tag{2.1}$$

subject to the dynamics,

$$\begin{aligned}
&\tfrac{d\mathcal{F}}{dt} = B - (\beta\mathcal{W} + g)F - \beta_1\mathcal{F}\mathcal{W} + \varepsilon_1\mathcal{P}_W - \gamma_1\mathcal{F} - \gamma_2\mathcal{F} + \varepsilon_2\mathcal{P}_I + \mathcal{U}_1\mathcal{W} - \mu\mathcal{F},\\
&\tfrac{d\mathcal{W}}{dt} = (\beta\mathcal{W} + g)\mathcal{F} + \beta_1\mathcal{F}\mathcal{W} - \delta_1\mathcal{W} + \delta_2\mathcal{I} - \eta_1\mathcal{W} - \mathcal{U}_1\mathcal{W} - \mathcal{U}_2\mathcal{W} - \mu\mathcal{W},\\
&\tfrac{d\mathcal{I}}{dt} = -Q\mathcal{I} + \delta_1\mathcal{W} - \delta_2\mathcal{I} - \eta_2\mathcal{I} - \mathcal{U}_3\mathcal{I} - \mu\mathcal{I},\\
&\tfrac{d\mathcal{P}_W}{dt} = \eta_1\mathcal{W} - \varepsilon_1\mathcal{P}_W + \gamma_1\mathcal{F} + \mathcal{U}_2\mathcal{W} - \mu_{\mathcal{W}}\mathcal{P}_W,\\
&\tfrac{d\mathcal{P}_I}{dt} = \eta_2\mathcal{I} - \varepsilon_2\mathcal{P}_I + \gamma_2\mathcal{F} + \mathcal{U}_3\mathcal{I} - \mu_I\mathcal{P}_I,
\end{aligned} \tag{2.2}$$

Table 1. Notation and parametric values.

Notation	Description	Parametric value
B	Compactness level of forest resources	100
Q	The constant rate of resources provided to non-wood based industries which are independent of forest resources	0.6
g	movement of wood-based industries to the forest region, which directly depends on the density of forest resources	0.8
β	The rate of decline of forest resources caused by wood-based industries	0.04
β_1	The growth rate of wood-based industries attributed to forest resources	0.003
μ	The natural depletion rate	1
μ_W	The natural depletion rate of pollutants released by wood-based industries	1
μ_I	The natural depletion rate of pollutants released by non-wood-based industries	1
δ_1	The rate of competition effects of $\mathcal{I}$ on $\mathcal{W}$	0.5
δ_2	The rate of competition effects of $\mathcal{W}$ on $\mathcal{I}$	0.3
ε_1	The loss of pollutants generated by wood-based industries due to forest resources	0.02
ε_2	The loss of pollutants generated by non-wood-based industries due to forest resources	0.01
γ_1	Depletion rate of forest resources due to the pollutants generated through wood-based industries	0.5
γ_2	Depletion rate of forest resources due to pollutants from non-wood industries	0.5
η_1	Increased rate of wood based pollutant emissions from industries	0.1
η_2	Increased rate of pollutant emissions from non-wood sources in industries	0.7

where $\mathcal{F}, \mathcal{W}, \mathcal{I}, \mathcal{P}_W, \mathcal{P}_I \geq 0$.

The proposed model includes five distinct compartments: forest resource density ($\mathcal{F}$), wood-based industry density ($\mathcal{W}$), non-wood-based industry density ($\mathcal{I}$), pollutants from wood-based industries ($\mathcal{P}_W$), and pollutants from non-wood-based industries ($\mathcal{P}_I$). The control rate $\mathcal{U}_1$ is responsible for the reduction of wood-based industries to manage the use of forest resources. The control rates of $\mathcal{U}_2$ and $\mathcal{U}_3$ reduce pollutants from wood and non-wood based industries, respectively. The symbols, notations, and their values used in this mathematical model are presented below:

3. Preliminaries

In this section, we introduce SBPs and their operational matrix of the derivative, which in the numerical approach section 4, we use these polynomials to approximate the solutions of the problem of optimal control of the spread of forest pollution.

3.1. **Shifted Bernoulli polynomials.**

Shifted Bernoulli polynomials on the interval $[0, L]$ can be defined as follows:

$$\mathscr{B}_{i,L}(t) = \sqrt{\frac{2i+1}{L}} \sum_{k=0}^{i} (-1)^{i-k} \binom{i}{i-k} \binom{i+k}{k} \left(\frac{t}{L}\right)^k, i = 0, 1, \ldots \tag{3.1}$$

Here, $\mathfrak{B}_{N,L}(t)$ represents the vector of the first $N+1$ SBPs:

$$\mathfrak{B}_{N,L}(t) = [\mathscr{B}_{0,L}(t), \mathscr{B}_{0,L}(t), \ldots, \mathscr{B}_{N,L}(t)]^T. \tag{3.2}$$

Any function $u(t) \in \mathscr{L}^2[0, L]$ (subset the Hilbert space H) can be approximated by $u(t) \simeq \tilde{u}(t)$, where $\tilde{u}(t) \in \text{span}\{\mathscr{B}_{i,L}(t)\}$ [9]. This implies that for any $\nu(t) \in Y = \text{span}\{\mathscr{B}_{i,L}(t)\}$:

$$\| u(t) - \tilde{u}(t) \| \leq \| u(t) - \nu(t) \| . \tag{3.3}$$

Thus, $u(t)$ can be approximated as:

$$u(t) \simeq \tilde{u} = \sum_{i=0}^{N} u_i \mathscr{B}_{i,L}(t) = U^T \mathfrak{B}_{N,L}(t), \tag{3.4}$$

where $U = [u_0, u_1, u_2, \ldots, u_N]^T$, and u_i can be determined by by the formula

$$u_i = \int_0^L u(t)\mathscr{B}_{i,L}(t)dt, \ i = 0, 1, \ldots, N. \tag{3.5}$$

3.2. **SBPs Operational Matrix of the derivative.** The vector $\mathfrak{B}_{N,L}(t)$ presented in Eq. (3.2) has a derivative that can be expressed as follows:

$$\frac{d\mathfrak{B}_{N,L}(t)}{dt} = D^* \mathfrak{B}_{N,L}(t), \tag{3.6}$$

where D^* is the operational derivative matrix of size $(N+1) \times (N+1)$. In this section, we derive the matrix D^*. According to Eq. (3.3), each of component of the vector $\frac{d\mathfrak{B}_{N,L}(t)}{dt} \in H$ have a unique best approximation from the set Y. Therefore there is $B(t) = [b_0(t), b_1(t), \ldots, b_N(t)]^T$, $b_i(t) \in Y$, $i = 0, \cdots N$ as

$$\forall \nu(t) \in H, \ \| \frac{d\mathfrak{B}_{N,L}(t)}{dt} - B(t) \| \leq \| \frac{d\mathfrak{B}_{N,L}(t)}{dt} - \nu(t) \| . \tag{3.7}$$

Hence, we can deduce that

$$\forall \nu(t) \in H, \ < \frac{d\mathfrak{B}_{N,L}(t)}{dt} - B(t), \nu(t) >= 0, \tag{3.8}$$

where $\langle \cdot, \cdot \rangle$ denotes the inner product. Since $b_i(t) \in Y$, there exist unique coefficients $d_{i,j}$ for $i, j = 0, \ldots, N$ that can be shown as follows:

$$\begin{aligned} \frac{d\mathfrak{B}_{N,L}(t)}{dt} &= B(t) = [b_0(t), b_1(t), \ldots, b_N(t)]^T \\ &= \left[\sum_{j=0}^{N} d_{0,j}\mathscr{B}_{j,L}(t), \sum_{j=0}^{N} d_{1,j}\mathscr{B}_{j,L}(t), \ldots, \sum_{j=0}^{N} d_{N,j}\mathscr{B}_{j,L}(t) \right]^T = D^* \mathfrak{B}_{N,L}(t), \end{aligned}$$

where $D^* = [d_{i,j}]$ is a matrix of size $(N+1) \times (N+1)$. Using Eq. (3.8), we have:

$$< \frac{d\mathfrak{B}_{N,L}(t)}{dt} - D^* \mathfrak{B}_{N,L}(t), \mathfrak{B}_{N,L}(t) >= 0.$$

For clarity, we write:

$$D^* < \mathfrak{B}_{N,L}(t), \mathfrak{B}_{N,L}(t) >=< \frac{d\mathfrak{B}_{N,L}(t)}{dt}, \mathfrak{B}_{N,L}(t) >, \tag{3.9}$$

where $\langle \mathfrak{B}_{N,L}(t), \mathfrak{B}_{N,L}(t) \rangle$ is a matrix of size $(N+1) \times (N+1)$. Let

$$D =< \mathfrak{B}_{N,L}(t), \mathfrak{B}_{N,L}(t) >= \int_0^L \mathfrak{B}_{N,L}(t)\mathfrak{B}_{N,L}^T(t)dt. \tag{3.10}$$

Therefore, the function $\frac{d\mathfrak{B}_{N,L}(t)}{dt}$ can be expanded in SBPs as follows:

$$\frac{d\mathfrak{B}_{N,L}(t)}{dt} = D^* \mathfrak{B}_{N,L}(t),$$

from which, using Eqs. (3.9) and (3.10), we have:

$$D^* =< \frac{d\mathfrak{B}_{N,L}(t)}{dt}, \mathfrak{B}_{N,L}(t) > D^{-1}.$$

4. Numerical Approach

Using the SBPs, we can approximate our unknown functions within Problem $\mathcal{A}$ as follows:

$$\begin{aligned}
&\mathcal{F}(t) \simeq \kappa_1^T \mathfrak{B}_{N,L}(t), \quad \mathcal{W}(t) \simeq \kappa_2^T \mathfrak{B}_{N,L}(t), \quad \mathcal{I}(t) \simeq \kappa_3^T \mathfrak{B}_{N,L}(t),\\
&\mathcal{P}_W(t) \simeq \kappa_4^T \mathfrak{B}_{N,L}(t), \quad \mathcal{P}_I(t) \simeq \kappa_5^T \mathfrak{B}_{N,L}(t), \quad \mathcal{U}_1(t) \simeq \kappa_6^T \mathfrak{B}_{N,L}(t),\\
&\mathcal{U}_2(t) \simeq \kappa_7^T \mathfrak{B}_{N,L}(t), \quad \mathcal{U}_3(t) \simeq \kappa_8^T \mathfrak{B}_{N,L}(t),
\end{aligned} \tag{4.1}$$

in which $\kappa_i,\ i = 1, \ldots, 8$ are

$$\begin{aligned}
&\kappa_1 = [k_0, \ldots, k_N]^T, \quad \kappa_2 = [k_{N+1}, \ldots, k_{2N+1}]^T, \quad \kappa_3 = [k_{2N+2}, \ldots, k_{3N+2}]^T,\\
&\kappa_4 = [k_{3N+3}, \ldots, k_{4N+3}]^T, \quad \kappa_5 = [k_{4N+4}, \ldots, k_{5N+4}]^T. \quad \kappa_6 = [k_{5N+5}, \ldots, k_{6N+5}]^T\\
&\kappa_7 = [k_{6N+6}, \ldots, k_{7N+6}]^T, \quad \kappa_8 = [k_{7N+7}, \ldots, k_{8N+7}]^T.
\end{aligned}$$

By using Eqs. (3.6) and (4.1), we have

$$\begin{aligned}
&\tfrac{d\mathcal{F}(t)}{dt} \simeq \kappa_1^T D^* \mathfrak{B}_{N,L}(t), \quad \tfrac{d\mathcal{W}(t)}{dt} \simeq \kappa_2^T D^* \mathfrak{B}_{N,L}(t), \quad \tfrac{d\mathcal{I}(t)}{dt} \simeq \kappa_3^T D^* \mathfrak{B}_{N,L}(t),\\
&\tfrac{d\mathcal{P}_W(t)}{dt} \simeq \kappa_4^T D^* \mathfrak{B}_{N,L}(t), \quad \tfrac{d\mathcal{P}_I(t)}{dt} \simeq \kappa_5^T D^* \mathfrak{B}_{N,L}(t).
\end{aligned} \tag{4.2}$$

By substituting Equations (4.1) and (4.2) in system dynamics (2.2), we have 5 equations and $(8N + 8)$ unknowns of k_i. By substituting the initial conditions

$$\mathcal{F}(0) = \mathcal{F}_0 = 10, \quad \mathcal{W}(0) = \mathcal{W}_0 = 8, \quad \mathcal{I}(0) = \mathcal{I}_0 = 7, \quad \mathcal{P}_W(0) = \mathcal{P}_{W0} = 3, \quad \mathcal{P}_I(0) = \mathcal{P}_{I0} = 1,$$

in equations (4.1), we can obtain 5 equations as follows:

$$\begin{aligned}
&\mathcal{F}_0 = \kappa_1^T \mathfrak{B}_{N,L}(0), \quad \mathcal{W}_0 = \kappa_2^T \mathfrak{B}_{N,L}(0), \quad \mathcal{I}_0 = \kappa_3^T \mathfrak{B}_{N,L}(0),\\
&\mathcal{P}_{W0} = \kappa_4^T \mathfrak{B}_{N,L}(0), \quad \mathcal{P}_{I0} = \kappa_5^T \mathfrak{B}_{N,L}(0).
\end{aligned}$$

By collocating the equations in constraints of problem $\mathcal{A}$ at N Gauss-Legendre (GL) nodes τ_i, we obtain $5N$ total equations

$$\begin{aligned}
\kappa_1^T D^* \mathfrak{B}_{N,L}(\tau_i) &= B - (\beta(\kappa_2^T \mathfrak{B}_{N,L}(\tau_i)) + g)(\kappa_1^T \mathfrak{B}_{N,L}(\tau_i)) - \beta_1(\kappa_1^T \times \kappa_2^T)\mathfrak{B}_{N,L}(\tau_i) + \varepsilon_1(\kappa_4^T \mathfrak{B}_{N,L}(\tau_i))\\
&\quad - \gamma_1(\kappa_1^T \mathfrak{B}_{N,L}(\tau_i)) - \gamma_2(\kappa_1^T \mathfrak{B}_{N,L}(\tau_i)) + \varepsilon_2(\kappa_5^T \mathfrak{B}_{N,L}(\tau_i)) + (\kappa_6^T \times \kappa_2^T)\mathfrak{B}_{N,L}(\tau_i) - \mu(\kappa_1^T \mathfrak{B}_{N,L}(\tau_i)),\\
\kappa_2^T D^* \mathfrak{B}_{N,L}(\tau_i) &= (\beta(\kappa_2^T \mathfrak{B}_{N,L}(\tau_i)) + g)(\kappa_1^T \mathfrak{B}_{N,L}(\tau_i)) + \beta_1(\kappa_1^T \times \kappa_2^T)\mathfrak{B}_{N,L}(\tau_i)) - \delta_1(\kappa_2^T \mathfrak{B}_{N,L}(\tau_i))\\
&\quad + \delta_2 \kappa_3^T \mathfrak{B}_{N,L}(\tau_i) - \eta_1(\kappa_2^T \mathfrak{B}_{N,L}(\tau_i)) - (\kappa_6^T \times \kappa_2^T)\mathfrak{B}_{N,L}(\tau_i) - (\kappa_7^T \times \kappa_2^T)\mathfrak{B}_{N,L}(\tau_i) - \mu(\kappa_2^T \mathfrak{B}_{N,L}(\tau_i)),\\
\kappa_3^T D^* \mathfrak{B}_{N,L}(\tau_i) &= -Q\kappa_3^T \mathfrak{B}_{N,L}(\tau_i) + \delta_1(\kappa_2^T \mathfrak{B}_{N,L}(\tau_i)) - \delta_2 \kappa_3^T \mathfrak{B}_{N,L}(\tau_i) - \eta_2 \kappa_3^T \mathfrak{B}_{N,L}(\tau_i)\\
&\quad - (\kappa_8^T \times \kappa_3^T)\mathfrak{B}_{N,L}(\tau_i) - \mu\kappa_3^T \mathfrak{B}_{N,L}(\tau_i),\\
\kappa_4^T D^* \mathfrak{B}_{N,L}(\tau_i) &= \eta_1(\kappa_2^T \mathfrak{B}_{N,L}(t)) - \varepsilon_1 \kappa_4^T \mathfrak{B}_{N,L}(\tau_i) + \gamma_1(\kappa_1^T \mathfrak{B}_{N,L}(\tau_i)) + (\kappa_7^T \times \kappa_2^T)\mathfrak{B}_{N,L}(\tau_i) - \mu_W \kappa_4^T \mathfrak{B}_{N,L}(\tau_i),\\
\kappa_5^T D^* \mathfrak{B}_{N,L}(\tau_i) &= \eta_2 \kappa_3^T \mathfrak{B}_{N,L}(\tau_i) - \varepsilon_2 \kappa_5^T \mathfrak{B}_{N,L}(\tau_i) + \gamma_2(\kappa_1^T \mathfrak{B}_{N,L}(\tau_i)) + (\kappa_8^T \times \kappa_3^T)\mathfrak{B}_{N,L}(\tau_i) - \mu_I \kappa_5^T \mathfrak{B}_{N,L}(\tau_i).
\end{aligned} \tag{4.3}$$

The equations now give $(5N + 5)$ nonlinear algebraic equations. Gauss-Legendre quadrature is used after appropriate transformations to approximate the value function given in (2.1), as follows:

$$\begin{aligned}
\mathcal{J} &= \int_0^L \Big(A_1\mathcal{F}^2(t) + A_2\mathcal{W}^2(t) + A_3\mathcal{I}^2(t) + A_4\mathcal{P}_w^2(t) + A_5\mathcal{P}_I^2(t) + \omega_1\mathcal{U}_1^2(t) + \omega_2\mathcal{U}_2^2(t) + \omega_3\mathcal{U}_3^2(t)\Big)dt\\
&= \frac{L}{2}\int_{-1}^{1} \Big(A_1\mathcal{F}^2(\frac{L(\eta+1)}{2}) + A_2\mathcal{W}^2(\frac{L(\eta+1)}{2}) + A_3\mathcal{I}^2(\frac{L(\eta+1)}{2}) + A_4\mathcal{P}_w^2(\frac{L(\eta+1)}{2}) + A_5\mathcal{P}_I^2(\frac{L(\eta+1)}{2})\Big)d\eta\\
&= \frac{L}{2}\sum_{i=1}^{N} \varpi_i\Big(A_1\mathcal{F}^2(\frac{L(\eta_i+1)}{2}) + A_2\mathcal{W}^2(\frac{L(\eta_i+1)}{2}) + A_3\mathcal{I}^2(\frac{L(\eta_i+1)}{2})\\
&\quad + A_4\mathcal{P}_w^2(\frac{L(\eta_i+1)}{2}) + A_5\mathcal{P}_I^2(\frac{L(\eta_i+1)}{2}) + \omega_1\mathcal{U}_1^2(\frac{L(\eta_i+1)}{2}) + \omega_2\mathcal{U}_2^2(\frac{L(\eta_i+1)}{2}) + \omega_3\mathcal{U}_3^2(\frac{L(\eta_i+1)}{2})\Big),
\end{aligned} \tag{4.4}$$

where η_i's are the zero point of the Legendre polynomial $\mathcal{L}_N(t)$ at $[-1,1]$, and ϖ_i's are the corresponding weights. The quadrature weight ϖ_i can be obtained from the following relationship [11]:

$$\varpi_i = \frac{2}{(1-\eta_i^2)[\mathcal{L}'_N(\eta_i)]^2}. \tag{4.5}$$

At last, the problem $\mathcal{A}$ is converted to problem $\mathcal{A}_N$ as follows:
Problem $\mathcal{A}_N$: Find κ_i for $i = 0, \cdots, 8N+7$ that minimize

$$\begin{aligned} J_N = \frac{L}{2}\sum_{i=1}^{N} \varpi_i \Big(& A_1\mathcal{F}^2(\frac{L(\eta_i+1)}{2}) + A_2\mathcal{W}^2(\frac{L(\eta_i+1)}{2}) + A_3\mathcal{I}^2(\frac{L(\eta_i+1)}{2}) + A_4\mathcal{P}_w^2(\frac{L(\eta_i+1)}{2}) \\ & + A_5\mathcal{P}_I^2(\frac{L(\eta_i+1)}{2}) + \omega_1\mathcal{U}_1^2(\frac{L(\eta_i+1)}{2}) + \omega_2\mathcal{U}_2^2(\frac{L(\eta_i+1)}{2}) + \omega_3\mathcal{U}_3^2(\frac{L(\eta_i+1)}{2})\Big), \end{aligned} \tag{4.6}$$

subject to

$$\begin{cases} \kappa_1^T D^*\mathfrak{B}_{N,L}(\tau_i) = B - (\beta(\kappa_2^T\mathfrak{B}_{N,L}(\tau_i)) + g)(\kappa_1^T\mathfrak{B}_{N,L}(\tau_i)) - \beta_1(\kappa_1^T \times \kappa_2^T)\mathfrak{B}_{N,L}(\tau_i) + \varepsilon_1(\kappa_4^T\mathfrak{B}_{N,L}(\tau_i)) \\ \qquad - \gamma_1(\kappa_1^T\mathfrak{B}_{N,L}(\tau_i)) - \gamma_2(\kappa_1^T\mathfrak{B}_{N,L}(\tau_i)) + \varepsilon_2(\kappa_5^T\mathfrak{B}_{N,L}(\tau_i)) + (\kappa_6^T \times \kappa_2^T)\mathfrak{B}_{N,L}(\tau_i) \\ \qquad - \mu(\kappa_1^T\mathfrak{B}_{N,L}(\tau_i)), \\ \kappa_2^T D^*\mathfrak{B}_{N,L}(\tau_i) = (\beta(\kappa_2^T\mathfrak{B}_{N,L}(\tau_i)) + g)(\kappa_1^T\mathfrak{B}_{N,L}(\tau_i)) + \beta_1(\kappa_1^T \times \kappa_2^T)\mathfrak{B}_{N,L}(\tau_i)) - \delta_1(\kappa_2^T\mathfrak{B}_{N,L}(\tau_i)) \\ \qquad + \delta_2\kappa_3^T\mathfrak{B}_{N,L}(\tau_i) - \eta_1(\kappa_2^T\mathfrak{B}_{N,L}(\tau_i)) - (\kappa_6^T \times \kappa_2^T)\mathfrak{B}_{N,L}(\tau_i) - (\kappa_7^T \times \kappa_2^T)\mathfrak{B}_{N,L}(\tau_i) \\ \qquad - \mu(\kappa_2^T\mathfrak{B}_{N,L}(\tau_i)), \\ \kappa_3^T D^*\mathfrak{B}_{N,L}(\tau_i) = -Q\kappa_3^T\mathfrak{B}_{N,L}(\tau_i) + \delta_1(\kappa_2^T\mathfrak{B}_{N,L}(\tau_i)) - \delta_2\kappa_3^T\mathfrak{B}_{N,L}(\tau_i) - \eta_2\kappa_3^T\mathfrak{B}_{N,L}(\tau_i) \\ \qquad - (\kappa_8^T \times \kappa_3^T)\mathfrak{B}_{N,L}(\tau_i) - \mu\kappa_3^T\mathfrak{B}_{N,L}(\tau_i), \\ \kappa_4^T D^*\mathfrak{B}_{N,L}(\tau_i) = \eta_1(\kappa_2^T\mathfrak{B}_{N,L}(t)) - \varepsilon_1\kappa_4^T\mathfrak{B}_{N,L}(\tau_i) + \gamma_1(\kappa_1^T\mathfrak{B}_{N,L}(\tau_i)) + (\kappa_7^T \times \kappa_2^T)\mathfrak{B}_{N,L}(\tau_i) \\ \qquad - \mu_W\kappa_4^T\mathfrak{B}_{N,L}(\tau_i), \\ \kappa_5^T D^*\mathfrak{B}_{N,L}(\tau_i) = \eta_2\kappa_3^T\mathfrak{B}_{N,L}(\tau_i) - \varepsilon_2\kappa_5^T\mathfrak{B}_{N,L}(\tau_i) + \gamma_2(\kappa_1^T\mathfrak{B}_{N,L}(\tau_i)) + (\kappa_8^T \times \kappa_3^T)\mathfrak{B}_{N,L}(\tau_i) - \mu_I\kappa_5^T\mathfrak{B}_{N,L}(\tau_i). \end{cases} \tag{4.7}$$

When the continuous problem $\mathcal{A}$ is discretized, it converts the infinite-dimensional problem $\mathcal{A}$ into a finite-dimensional nonlinear optimization problem, referred to as $\mathcal{A}_N$. Various advanced NLP techniques are available to solve this problem [10]. The method for solving the nonlinear constrained optimization problem involves the sequential quadratic programming (SQP) algorithm, which is an iterative technique for nonlinear optimization [10].

5. Convergence analysis

To facilitate the convergence analysis, we reformulate the problem $\mathcal{A}$ in a vectorial framework, thereby enabling a more succinct and generalized examination of the underlying mathematical structure. Let

$$x'(t) = F(x(t), u(t)), \tag{5.1}$$

where $x(t) = (\mathcal{F}(t), \mathcal{W}(t), \mathcal{I}(t), \mathcal{P}_w(t), \mathcal{P}_I(t))$ and $u(t) = (\mathcal{U}_1(t), \mathcal{U}_2(t), \mathcal{U}_3(t))$ be state and control vectors of problem $\mathcal{A}$. Here, $F(x(t), u(t))$ is as following

$$F(x(t), u(t)) = \begin{bmatrix} B - (\beta\mathcal{W} + g)\mathcal{F} - \beta_1\mathcal{F}\mathcal{W} + \varepsilon_1\mathcal{P}_W - \gamma_1\mathcal{F} - \gamma_2\mathcal{F} + \varepsilon_2\mathcal{P}_I + \mathcal{U}_1\mathcal{W} - \mu\mathcal{F}, \\ (\beta\mathcal{W} + g)\mathcal{F} + \beta_1\mathcal{F}\mathcal{W} - \delta_1\mathcal{W} + \delta_2\mathcal{I} - \eta_1\mathcal{W} - \mathcal{U}_1\mathcal{W} - \mathcal{U}_2\mathcal{W} - \mu\mathcal{W}, \\ -Q\mathcal{I} + \delta_1\mathcal{W} - \delta_2\mathcal{I} - \eta_2\mathcal{I} - \mathcal{U}_3\mathcal{I} - \mu\mathcal{I}, \\ \eta_1\mathcal{W} - \varepsilon_1\mathcal{P}_W + \gamma_1\mathcal{F} + u_2\mathcal{W} - \mu_W\mathcal{P}_W, \\ \eta_2\mathcal{I} - \varepsilon_2\mathcal{P}_I + \gamma_2\mathcal{F} + \mathcal{U}_3\mathcal{I} - \mu_I\mathcal{P}_I \end{bmatrix}.$$

Let $x_N^*(t) = (\mathcal{F}_N^*(t), \mathcal{W}_N^*(t), \mathcal{I}_N^*(t), \mathcal{P}_{wN}^*(t), \mathcal{P}_{IN}^*(t))$ and $u_N^*(t) = (\mathcal{U}_{1N}^*(t), \mathcal{U}_{2N}^*(t), \mathcal{U}_{3N}^*(t))$ be an optimal solution of problem $\mathcal{A}_N$. Also, let

$$x_N(t) = (\kappa_1^T\mathcal{B}_{N,L}(t), \kappa_2^T\mathcal{B}_{N,L}(t), \kappa_3^T\mathcal{B}_{N,L}(t), \kappa_4^T\mathcal{B}_{N,L}(t), \kappa_5^T\mathcal{B}_{N,L}(t)),$$

is N-th order of approximation x_N^* and $u_N(t)$ is any approximation of $u_N^*(t)$, where $\mathcal{B}_{N,L}(t)$ is the vector of SBPs defined by (3.1). It is worth mentioning that $\mathcal{B}_{N,L}(t)$ can be any other orthogonal polynomials. We now consider a sequence of problems $\mathcal{A}_N$, where N ranges from N_1 to infinity. Consequently, we obtain a sequence of discrete optimal solutions $\{(x_i^*, u_i^*) : i = 1, \cdots, N\}_{N=N_1}^{\infty}$ and their corresponding approximation functions $\{(x_N, u_N)\}_{N=N_1}^{\infty}$. Theorem 5.1 demonstrates that if problem $\mathcal{A}$ has feasible solutions, then problem $\mathcal{A}_N$ also has feasible solutions.

Theorem 5.1. *Given that (x, u) are feasible solutions for Problem $\mathcal{A}$ and that the state function $x(t)$ lies within a Sobolev space $W^{m,\infty}$ where $m \geq 2$, for sufficiently large N, Problem $\mathcal{A}_N$ has a feasible solution $(\bar{x}_i, \bar{u}_i)$. Here, $\bar{u}_i = u(s_i)$ and*

$$||x(s_i) - \bar{x}_i||_\infty \leq M(N-1)^{1-m}, \qquad 1 \leq i \leq N. \tag{5.2}$$

The nodes s_i are Legendre-Gauss-Lobatto points, and M is a positive constant independent of N [4].

Theorem 5.1 ensures the existence of high-quality feasible solutions for Problem $\mathcal{A}_N$ when N is sufficiently large, with the control variables closely approximating the true control function and the state variables being close to the true state trajectory. The following theorem is important because it provides a theoretical guarantee that the pseudospectral method, which discretizes the optimal control problem, can be used to reliably approximate the solution of the original continuous problem. The Following lemma and definition are utilized in Theorem 5.4.

Lemma 5.2. *Let $\tau_j, j = 1, \ldots, N$ be the nodes of the G-L quadrature and w_j the associated weights. If the function $f(t)$ is Riemann integrable, then we have:*

$$\int_{-1}^{1} f(t)\, dt = \lim_{N\to\infty} \sum_{j=1}^{N} f(\tau_j) w_j.$$

This result states that for a Riemann integrable function $f(t)$, the sum of the function's values at the G-L nodes, weighted by their respective weights, converges to the integral of $f(t)$ over the interval $[-1, 1]$ as N approaches infinity.

Definition 5.3. A continuous function $\zeta(t)$ is described as a uniform accumulation point of the sequence $\{\zeta_N(t)\}_{N=1}^{\infty}$ on the interval $t \in [-1, 1]$, if a subsequence of $\{\zeta_N(t)\}_{N=1}^{\infty}$ exists that converges uniformly to $\zeta(t)$.

Theorem 5.4. *Consider the sequence $\{(x_i^*, u_i^*), 1 \leq i \leq N\}_{N=N_1}^{\infty}$, which represents the optimal solutions for the discretized problem A_N. Additionally, let $\{(x_N(t), u_N(t))\}_{N=N_1}^{\infty}$ denote the corresponding sequence of interpolated functions. Suppose $(q(t), u(t))$ is any accumulation point of the sequence $\{(x'_N(t), u_N(t))\}_{N=N_1}^{\infty}$ in a uniform sense. Then $p(t)$ will be an optimal control for the original continuous problem A, and $x(t)$ that satisfies*

$$x(t) = \int_0^t q(\tau) d\tau + x(0),$$

will be the associated optimal trajectory.

This theorem confirms that, under specific conditions, the sequence of solutions derived from the discretized problem A_N converges to the solution of the original continuous problem A.

The following lemma provides a bound for the approximation error when a function $f(t)$ in $C^{N+1}[0, L]$ is approximated by the best approximation from a space spanned by a set of basis functions, demonstrating that the error decreases as the number of basis functions increases.

Lemma 5.5. *Let $f(t)$ be a function that belongs to the space $C^{N+1}[0, L]$. Assume S_N is the span of the set of functions $\{\mathscr{B}_{0,L}(t), \mathscr{B}_{1,L}(t), \ldots, \mathscr{B}_{N,L}(t)\}$. If $C^T \mathfrak{B}_{N,L}(t)$ is the best approximation of $f(t)$ within S_N, then the following inequality holds:*

$$\|f(t) - C^T \mathfrak{B}_{N,L}(t)\|_{\mathscr{L}^2[0,L]} \leq \frac{K^2 L^{2N+3}}{(N+1)!^2(2N+3)},$$

where K is defined as $\max_{t\in[0,L]} |f^{(N+1)}(t)|$.

Proof. Given that the set $\{1, t, \ldots, t^N\}$ forms a basis for the space of polynomials of degree N, we define:

$$y_1(t) = f(0) + tf'(0) + \frac{t^2}{2!}f''(0) + ... + \frac{t^N}{N!}f^{(N)}(0).$$

From the Taylor series expansion, the difference between $f(t)$ and $y_1(t)$ can be expressed as:

$$|f(t) - y_1(t)| = \left|\frac{f^{(N+1)}(\xi_t)t^{N+1}}{(N+1)!}\right|,$$

where ξ_t is some value in the interval (0, L). Since $C^T\mathfrak{B}_{N,L}(t)$ is the best approximation of $f(t)$ within S_N, and $y_1(t)$ is an element of S_N, we can assert:

$$\|f(t) - C^T\mathfrak{B}_{N,L}(t)\|^2_{\mathscr{L}^2[0,L]} \leq \|f(t) - y_1(t)\|^2_{\mathscr{L}^2[0,L]}.$$

This leads to:

$$\int_0^L |f(t) - y_1(t)|^2 dt = \int_0^L \left|\frac{f^{(N+1)}(\xi_t)t^{N+1}}{(N+1)!}\right|^2 dt \leq \frac{K^2}{(N+1)!^2}\int_0^L t^{2N+2}dt = \frac{K^2L^{2N+3}}{(N+1)!^2(2N+3)}.$$

Taking the square root completes the proof, establishing the required bound. □

6. Numerical Simulation

The numerical simulations conducted in Wolfram Mathematica R2017a on a 64-bit computer with an Intel Core i7 processor (1.6GHz) and 4GB of RAM investigated the optimal control for pollutant spread through forest resources based on SBPs. The parameter values used in the simulations are provided in Table 1, which are referenced from [17]. The behavior of the optimal control for pollutant spread through forest resources is illustrated in Figures 1–8. In these figures, the unit of the time axis is in decades.

Figure 1 shows the forest resource density over time. The graph shows that the density of forest resources starts high at $t = 0$ but declines steadily over time. Around $t = 5$, there is a significant drop, likely due to the cumulative effects of pollution and resource depletion. Towards $t = 20$, the density stabilizes at a lower value, suggesting that the forest resources have reached a new equilibrium or that the maximum impact of control measures has been achieved. The decrease in forest resources is directly related to the increase in pollution from wood-based and non-wood industries, which is observable in Figures 4 and 5. Figure 2 demonstrates wood-based industry density over time. Initially, the density of wood-based industries is moderate but increases sharply, peaking around $t = 5$, which indicates rapid industrial growth. Following this peak, there is a gradual decline, and the density stabilizes around $t = 15$, possibly due to the implementation of regulatory controls or resource depletion. The increase in the density of wood based industries can lead to an increase in pollution emissions, as observed in Figure 4 from wood-based industry pollution. Figure 3 shows non-wood-based industry density over time. The density of non-wood-based industries starts low and increases steadily throughout the time period. This figure is approximately similar to the wood-based industries figure, but the density of non-wood industries is lower. This shows that the activities of non-wood industries are fewer compared to wood-based industries. Similar to wood-based industries, the increase in the density of non-wood industries can also lead to an increase in pollution emissions, as observed in the graph related to pollution from non-wood industries in Figure 5.

Figure 4 shows pollutants from wood-based industries over time. Pollutant levels from wood-based industries begin low but increase sharply with industrial activity. The pollutant levels peak in correlation with the peak in industry density and then decline, approximately stabilizing after $t = 15$. This pattern suggests that control measures have been effective in reducing pollutants from these industries. The increase in pollution from wood-based industries can lead to a reduction in forest resources, as observed in the forest density Figure 1. Figure 5 demonstrates pollutants from non-wood-based industries over time. The pollutants from non-wood-based industries increase steadily until $t = 5$, and after that don't have a significant decline, reflecting the continuous growth of these industries and indicating a need for stricter pollution control measures. Similar to wood-based industries, the increase in pollution from non-wood industries can also lead to a reduction in forest resources, as seen in Figure 1.

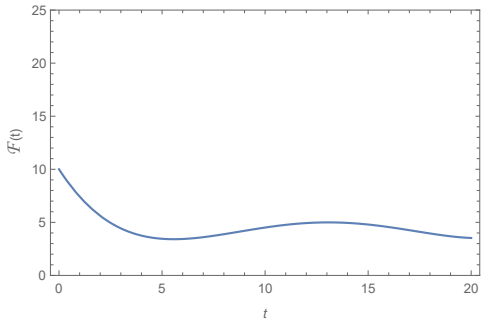

FIGURE 1. The density of forest resources.

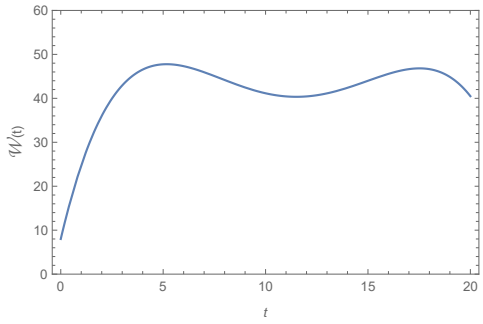

FIGURE 2. The density of wood-based industrial.

Figure 6, 7, and 8 are control effort $\mathcal{U}_1$, $\mathcal{U}_2$, and $\mathcal{U}_3$ over time. Figure 6 is dedicated to forest control and illustrates the optimal control behavior for forest resources. The graph in this figure depicts the changes in forest control ($\mathcal{U}_1$) over time t. At the beginning, $t = 0$, the control value is near zero. As time progresses, the control value becomes negative, reaching its lowest point around $t = 5$. After this point, the control value gradually increases, approaching zero around $t = 20$. This pattern indicates that, in the early stages of the study period, there is a greater need for control over the forest. This figure effectively demonstrates the dynamic behavior of optimal control for forest resource management, showing that timely and appropriate control measures can significantly aid in improving forest resources. Control measures can reduce pollution levels and stabilize forest resources. The graph of Figure 7 starts low and increases rapidly. This suggests a staggered implementation of control measures. After peaking around $t = 5$, $\mathcal{U}_2$ also declines, then approximately stabilizes, indicating its effectiveness in pollutant control. Controls applied to non-wood industries can reduce pollution emissions and stabilize forest resources. Figure 8 is similar to the wood-based industries control figure, but at a lower level. Controls applied to non-wood industries can reduce pollution emissions and stabilize forest resources.

7. Conclusion

In this study, we presented a mathematical model to analyze the depletion of forest resources and the spread of pollutants through industrial activities. This model is based on optimal control governed by five ordinary differential equations. By applying numerical simulations based on the collocation method and using SBPs and their operational matrix of derivatives, we convert the original OCP into a NLP. We also demonstrated the effectiveness of various control strategies in mitigating the adverse effects of industrialization on forest ecosystems. The results highlight the importance of implementing sustainable practices and strict regulatory measures to conserve forest resources while balancing industrial growth. The convergence analysis of the method is also presented. The mathematical model and the associated numerical simulations provide a valuable framework for policymakers and environmental managers to evaluate and optimize strategies for forest conservation. Future work could extend this model by incorporating more complex interactions and feedback mechanisms, as well as exploring the socio-economic impacts of different conservation strategies. In summary, this research underscores the critical need for integrated approaches that combine mathematical modeling, numerical simulations, and practical policy measures to address the challenges of forest resource depletion and environmental pollution.

Acknowledgment

The authors are very grateful to the reviewers for carefully reading the paper and for their comments and suggestions, which have improved the paper. Also, this work has financial support from Farhangian University (Contract No. 50000.17474.120).

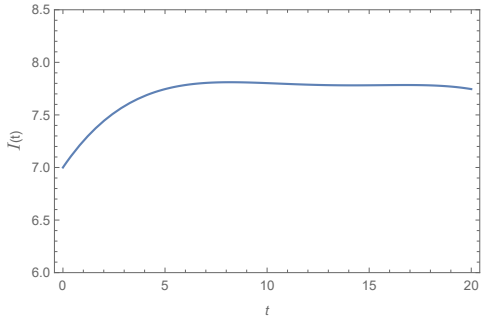

FIGURE 3. The density of non-wood-based industrial.

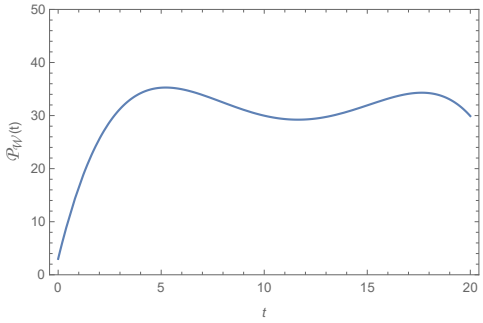

FIGURE 4. The pollutants through wood-based industries.

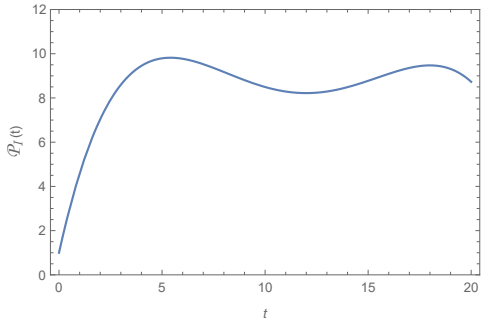

FIGURE 5. The pollutants through non-wood-based industries.

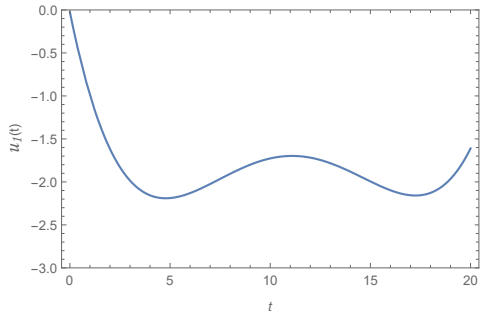

FIGURE 6. Forest control.

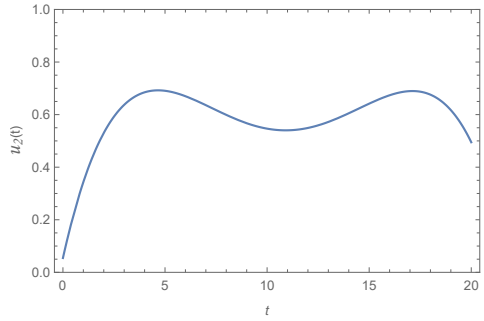

FIGURE 7. Wood-based industrial control.

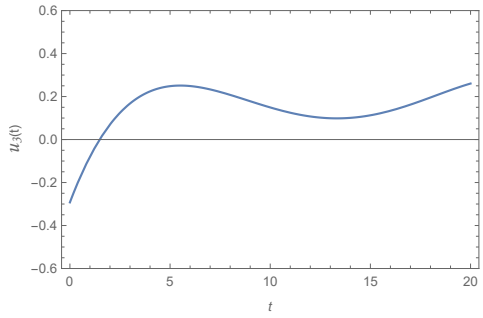

FIGURE 8. Non-wood-based industrial control.

CONFLICT OF INTEREST

The authors declare that they have no conflict of interest.

REFERENCES

[1] E. Buhe, M. Rafiullah, D. Jabeen, and N. Anjum, *Application of homotopy perturbation method to solve a nonlinear mathematical model of depletion of forest resources*, Frontiers in Physics, *11* (2023), 1246884.
[2] A. Eswari, S. V. Raj, and V. S. Priya, *Analysis of mathematical modeling the depletion of forestry resource: effects of population and industrialization*, Matrix Sci. Math., *3*(2) (2019), 22–26.
[3] G. Freud, *Orthogonal polynomials*, Pergamon Press, 1971.
[4] Q. Gong, I. M. Ross, W. Kang, and F. Fahroo, *On the pseudospectral covector mapping theorem for nonlinear optimal control*, in Proceedings of the 45th IEEE conference on decision and control, IEEE, (2006), 2679–2686.

[5] M. D. Goshu and M. F. Endalew, *Mathematical modeling on conservation of depleted forestry resources*, Nat. Resour. Model., *35*(2) (2022), e12338.
[6] E. Keshavarz, Y. Ordokhani, and M. Razzaghi, *A numerical solution for fractional optimal control problems via Bernoulli polynomials*, J. Vib. Control, *22*(18) (2016), 3889–3903.
[7] E. Keshavarz, Y. Ordokhani, and M. Razzaghi, *Bernoulli wavelet operational matrix of fractional order integration and its applications in solving the fractional order differential equations*, Appl. Math. Model., *38*(24) (2014), 6038–6051.
[8] R. Khanduzi, A. Ebrahimzadeh, and Z. Ebrahimzadeh, *A combined Bernoulli collocation method and imperialist competitive algorithm for optimal control of sediment in the dam reservoirs*, AUT J. Math. Comput., *5*(1) (2024), 71–80.
[9] E. Kreyszig, *Introductory Functional Analysis With Applications*, New York, John Wiley, 1978.
[10] D. G. Luenberger and Y. Ye, *Linear and nonlinear programming*, Springer, New York, 2008.
[11] K. Maleknejad and A. Ebrahimzadeh, *An efficient hybrid pseudo-spectral method for solving optimal control of Volterra integral systems*, Math. Commun. *19* (2014), 417–435.
[12] A. K. Misra and K. Lata, *Depletion and conservation of forestry resources: a mathematical model*, Diff. Equ. Dyn. Syst., *23* (2015), 25–41.
[13] C. Mohan, *Solution of real life optimization problems*, in Statistical modeling and applications on real-time problems, CRC Press, 2024, 152–170.
[14] S. Nemati and D. F. Torres, *Application of bernoulli polynomials for solving variable-order fractional optimal control-affine problems*, Axioms, *9*(4) (2020), 114.
[15] R. Pathak, *Depletion of forest resources and wildlife population with habitat complexity: A mathematical model*, Open J. of Ecol., *8*(11) (2018), 579.
[16] S. Qureshi and A. Yusuf, *Mathematical modeling for the impacts of deforestation on wildlife species using Caputo differential operator*, Chaos Solitons Fractals, *126* (2019), 32–40.
[17] N. H. Shah, M. H. Satia, and B. M. Yeolekar, *Optimum control for spread of pollutants through forest resources*, Appl. Math., *8*(5) (2017), 607–620.